The Company of
Biologists

RESEARCH ARTICLE

Delamination of neural crest cells requires transient and reversible Wnt inhibition mediated by Dact1/2

M. Angeles Rabadán[1], Antonio Herrera[2], Lucia Fanlo[1], Susana Usieto[1], Carlos Carmona-Fontaine[3], Elias H. Barriga[3], Roberto Mayor[3], Sebastián Pons[2] and Elisa Martí[1,*]

ABSTRACT

Delamination of neural crest (NC) cells is a bona fide physiological model of epithelial-to-mesenchymal transition (EMT), a process that is influenced by Wnt/β-catenin signalling. Using two *in vivo* models, we show that Wnt/β-catenin signalling is transiently inhibited at the time of NC delamination. In attempting to define the mechanism underlying this inhibition, we found that the scaffold proteins Dact1 and Dact2, which are expressed in pre-migratory NC cells, are required for NC delamination in *Xenopus* and chick embryos, whereas they do not affect the motile properties of migratory NC cells. Dact1/2 inhibit Wnt/β-catenin signalling upstream of the transcriptional activity of T cell factor (TCF), which is required for EMT to proceed. Dact1/2 regulate the subcellular distribution of β-catenin, preventing β-catenin from acting as a transcriptional co-activator to TCF, yet without affecting its stability. Together, these data identify a novel yet important regulatory element that inhibits β-catenin signalling, which then affects NC delamination.

KEY WORDS: Dishevelled antagonist of β-catenin, Dapper, Frodo, β-catenin, Nuclear bodies, *Xenopus* embryo, Chick embryo

INTRODUCTION

Epithelial-to-mesenchymal transition (EMT) is a process that has long been recognised as crucial for the generation of tissues and organs in both vertebrates and invertebrates. However, because EMT converts epithelial cells into migratory and invasive mesenchymal cells, it has also been established as an important step in the metastatic cascade of tumours (Nieto, 2013). To identify key molecular players in this process, we have studied the delamination of the neural crest (NC) as a bona fide *in vivo* model of physiological EMT. The NC is a population of cells that forms at the neural plate border of all vertebrate embryos and it gives rise to the peripheral nervous system, as well as to other derivatives such as cartilage, face and neck bone and muscle, pigmented cells in the skin, several endocrine glands and part of the heart (Mayor and Theveneau, 2013). Despite the fundamental role played by NC cells in the development of many tissues and organs, it remains unclear what controls the delamination and differentiation of these cells. Prior to delamination, NC progenitor

cells are specified by the sequential and coordinated activities of at least five different signalling pathways, the bone morphogenetic protein (BMP), Wnt, fibroblast growth factor (FGF), retinoic acid and Notch pathways (Betancur et al., 2010; Mayor and Theveneau, 2013; Streit and Stern, 1999). Indeed, inhibition of BMP and activation of Wnt signalling is required for the early stages of NC development. Although BMP activity and non-canonical Wnt signalling do appear to participate in NC delamination (Sela-Donenfeld and Kalcheim, 1999) and migration (De Calisto et al., 2005; Carmona-Fontaine et al., 2008; Mayor and Theveneau, 2014), respectively, how the pathways regulate these processes remains unclear.

To study NC delamination, we took advantage of two well-characterised models, *Xenopus* and chick embryos, to show that cell-autonomous inhibition of Wnt and β-catenin activity is a prerequisite for this process. To search for the mechanism underlying local Wnt inhibition, we performed a genome-wide expression screening of NC progenitors that identified dishevelled antagonist of β-catenin 2 (Dact2). Dact2 belongs to a small family of intracellular scaffold proteins (Dact1-Dact4; Schubert et al., 2014), which are nucleocytoplasmic proteins that were initially identified in *Xenopus* as dishevelled (Dsh)-interacting proteins that regulate Wnt activity by promoting degradation of Dsh (Cheyette et al., 2002; Gloy et al., 2002; Zhang et al., 2006). DACT proteins can also form complexes with β-catenin (Gao et al., 2008; Kivimäe et al., 2011; Wang et al., 2015), a key element in the canonical Wnt pathway (Clevers and Nusse, 2012). All vertebrates express at least one member of the DACT family in NC progenitors (Alvares et al., 2009; Hikasa and Sokol, 2004; Schubert et al., 2014), suggesting that they fulfil a conserved role in NC development. Here, we show that DACT proteins play a novel role in regulating the subcellular distribution of β-catenin, thereby impeding β-catenin from acting as a transcriptional co-activator to T cell factor (TCF). We also show that this inhibition is required for NC delamination. In light of these results, we propose a novel and reversible mechanism by which Wnt/β-catenin activity can be inhibited in a cell-autonomous manner – a mechanism that might be conserved in other physiological, as well as in pathological, Wnt-dependent processes.

RESULTS

Wnt/β-catenin signalling is transiently inhibited at the time of neural crest delamination

To begin to study the spatial regulation of Wnt activity during neural crest development *in vivo*, we first co-electroporated chick embryos at the 10 somite stage [Hamburger–Hamilton (HH) stage 10] with a Wnt-responsive reporter (TOP:H2B-RFP; Herrera et al., 2014) that serves as a readout of endogenous activation of the canonical Wnt pathway, together with a control vector stably expressing green fluorescent protein fused to histone H2B

[1]Department of Developmental Biology, Instituto de Biología Molecular de Barcelona, CSIC, Parc Científic de Barcelona, C/ Baldiri i Reixac 20, Barcelona 08028, Spain. [2]Department of Cell Biology, Instituto de Biología Molecular de Barcelona, CSIC, Parc Científic de Barcelona, C/Baldiri i Reixac 20, Barcelona 08028, Spain. [3]Department of Cell and Developmental Biology, University College London, Gower Street, London WC1E 6BT, UK.

*Author for correspondence (emgbmc@ibmb.csic.es)

E.M., 0000-0002-0411-0069

DEVELOPMENT

(pβActin-H2B-GFP; Fig. 1A). Canonical Wnt activity was spatially restricted to the dorsal neural tube (NT) 24 hours post-electroporation (hpe) (Fig. 1B). The temporal regulation of Wnt activity was studied by co-electroporation of the TOP:H2B-2dEGFP reporter, which has a 2 h half-life (Rios et al., 2010), along with the control pβActin-H2B-RFP vector. Activation of the Wnt/β-catenin pathway was then monitored by confocal microscopy and this activity was correlated with cell location and behaviour, as well as with the expression of the NC marker AP2 (Fig. 1C, see also Fig. S1A,B). We also analysed the GFP signal (normalised to RFP) within the dorsal NT cells and migratory NC cells. Although endogenous Wnt activity in neuroepithelial cells within the dorsal NT was quite variable, premigratory NC cells (AP2^{+}) exhibited weaker Wnt/β-catenin activity than neuroepithelial cells that are to remain within the neural tube (AP2^{−}; Fig. 1D,E). Moreover, early migratory NC cells still found close to the NT (<30 μm away) also exhibit weak Wnt/β-catenin reporter activity (Fig. 1D,E), whereas NC cells that have migrated away from the NT appear to have reactivated the Wnt pathway (Fig. 1D,E). Together, these observations show that premigratory NC cells inhibit endogenous canonical Wnt activity

at the time of their delamination but that migratory NC cells reactivate this pathway, prompting us to test whether this inhibition was a prerequisite for NC delamination.

To address this issue, we first electroporated a stable form of β-catenin into HH10 chick embryos in order to activate the Wnt pathway (Fig. 2A,B) and significantly impaired NC delamination at 24 hpe [Top-2dEGFP/RFP ratio (the ratio of co-electroporated cells co-expressing Top-2dEGFP and control RFP versus cells expressing only control RFP): 0.47±0.05 migratory cells; Fig. 2C-E,G]. Conversely, when the Wnt pathway was inhibited by electroporating the mutant Lrp6[ΔC] receptor (Fig. 2A,B), NC delamination was significantly enhanced at 24 hpe (ratio: 2.65±0.4 migratory cells; Fig. 2C-F,G). Moreover, injecting Wnt activators into one blastomere of an eight cell stage *Xenopus* embryo, restricted the extension of the cephalic NC migratory streams compared with that on the control uninjected side of the embryos (Fig. 2H). As in the chick embryos, inhibition of Wnt signalling augmented the extension of the cephalic NC migratory streams compared with that on the control side of the embryos (Fig. 2I). Together, these results indicated that Wnt signalling must be inhibited for NC cells to delaminate
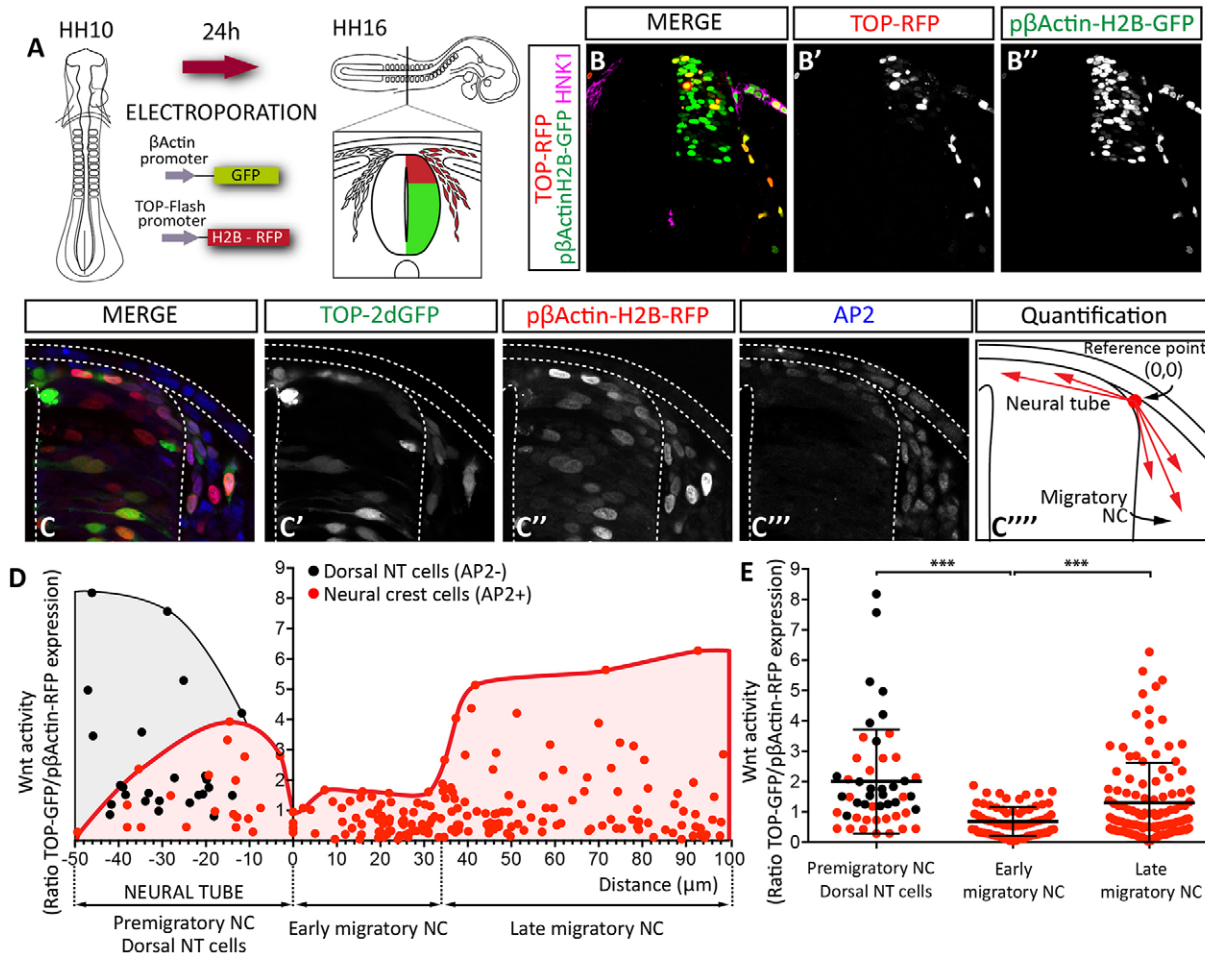

Fig. 1. Wnt/β-catenin activity is transiently inhibited at the time of delamination. (A) Scheme of the chick embryo electroporation at HH stage 10 to analyse TOP-RFP reporter expression. (B) Selected confocal images of chick embryo NT sections at 24 hpe with the indicated DNAs and immunostained with the NC marker Hnk1. Stabilised Wnt reporter (red) is activated in scattered cells in the dorsal NT. (C-C‴′) Selected confocal images of chick embryo NT sections 24 hpe with the indicated DNAs and immunostained with the NC marker AP2. (C′) Destabilised Wnt reporter activity (green). (C″) Control electroporation (red). (C‴) AP2 immunostaining (blue). (C‴′) Schematic representation depicts the reference point taken as zero distance to quantify the fluorescence intensity/cell at the distances indicated. (D) Quantification of the GFP/RFP fluorescence intensity ratio, where the dots represent individual cells at their given distance from zero. (E) Plots of the GFP/RFP fluorescence intensity ratio at three different distances from zero. The lines and error bars correspond to the median±s.e.m.; ***$P<0.001$, unpaired *t*-test (two-sided) (dorsal NT cells, ratio=2.0±1.7, n=49; early migratory NC cells, ratio=0.6±0.5, n=72; late migratory NC cells, ratio=1.3±1.3, n=119).
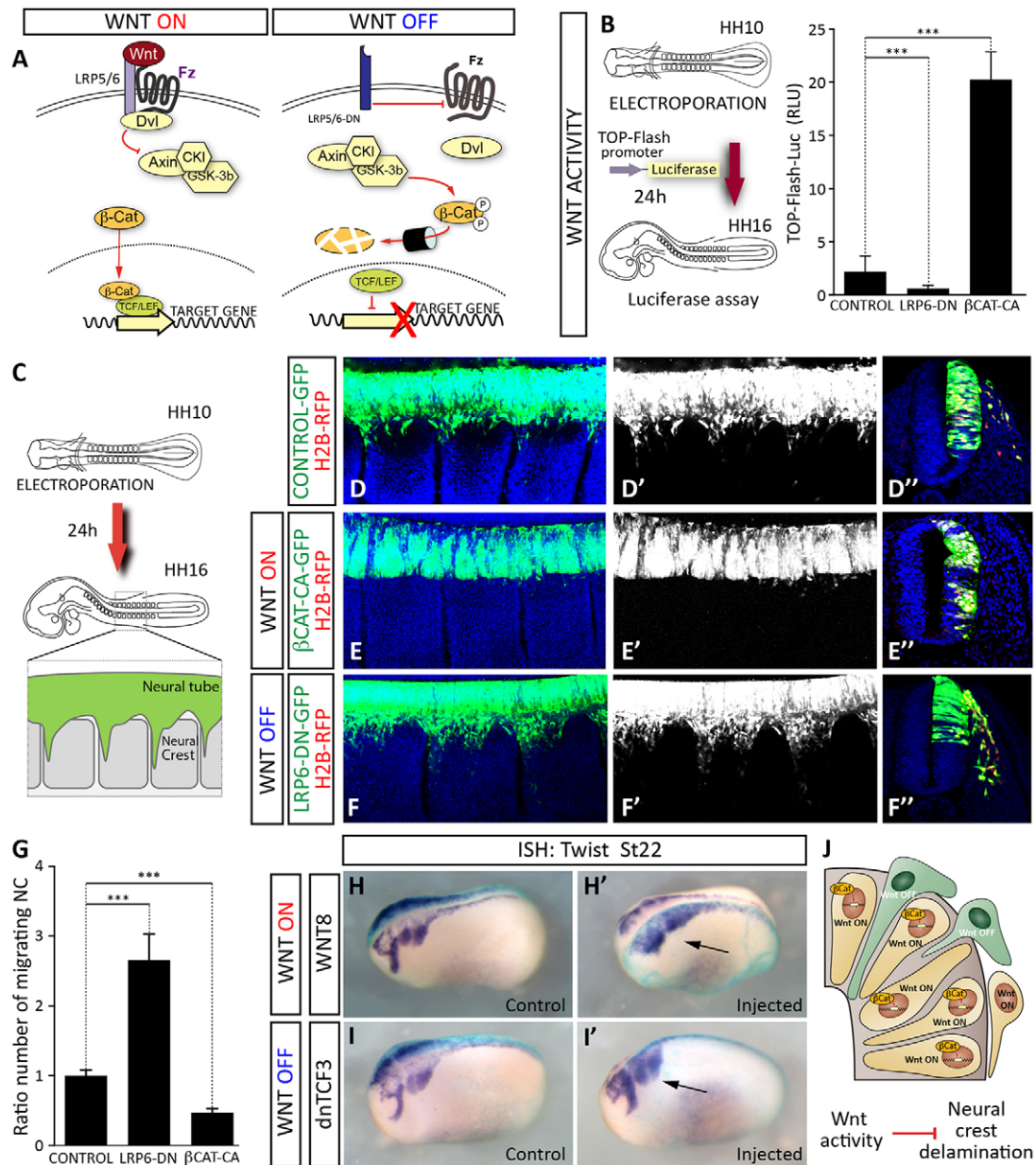
Fig. 2. Inhibition of the Wnt canonical pathway is required for NC delamination. (A) Scheme showing the components of the canonical Wnt pathway. (B) Scheme representing the TOP-Flash electroporation of chick embryos at HH10 for *in vivo* luciferase assays. Quantification of Luc/*Renilla* activity 24 hpe with the indicated DNAs. *Lrp6^{DN}* inhibits and β-catenin-CA activates the TOP-Flash reporter (mean±s.e.m., *n*=6-10 embryos/condition; ***$P<0.001$, one-way ANOVA). (C) Scheme showing the location of the transfected cells in chick embryos electroporated at HH10 (reporter GFP expression). (D-F) Selected images of embryos electroporated with DNA at HH10 in which GFP-expressing cell migration was analysed 24 hpe in whole-mount preparations. Lateral view shows the NC streams over 3 somites of the embryos. (D″, E″,F″) Selected transverse sections of electroporated NTs showing the migratory NC cells (green) in the three conditions co-stained with DAPI (blue). (G) Quantification of the EGFP-expressing cells (mean total±s.e.m. after electroporation, *n*=10-20 sections of ≥4 embryos/condition; ***$P<0.001$, one-way ANOVA). (H,I) *Xenopus laevis* embryos injected with RNA encoding Wnt8 (Wnt-ON) or dnTcf3 (Wnt-OFF) were fixed at stage 22. *In situ* hybridisation for *Xenopus twist1* shows that the cephalic NC streams have migrated less on the Wnt-ON injected side of the embryos whereas they have progressed further in the Wnt-OFF injected side of the embryos (*n*≥10/15 embryos/condition). (J) Schematic representation of pre-migratory NC cells in which activation of the Wnt pathway prevents delamination from the dorsal NT.

from the dorsal NT, prompting us to search for these inhibitory mechanisms (Fig. 2J).

Activity of Dact1/2 scaffold proteins is required for NC delamination

We used the BMP-responsive element (BRE-tk-GFP) that drives stable GFP expression in premigratory and early migratory NC cells to select and purify these cells, facilitating the search for new

regulators of NC development (Fig. 3A; see also Materials and Methods) (Rabadán et al., 2013). In this way, we identified Dact2, a protein belonging to a small family of intracellular scaffold proteins of which Dact1 (also named Frodo) and Dact2 are the closest family members (Schubert et al., 2014). Dact2 is the only family member expressed in the trunk NT of chick embryos where the premigratory NC cells reside (Alvares et al., 2009), whereas Dact1 is the only member expressed by NC progenitors in the
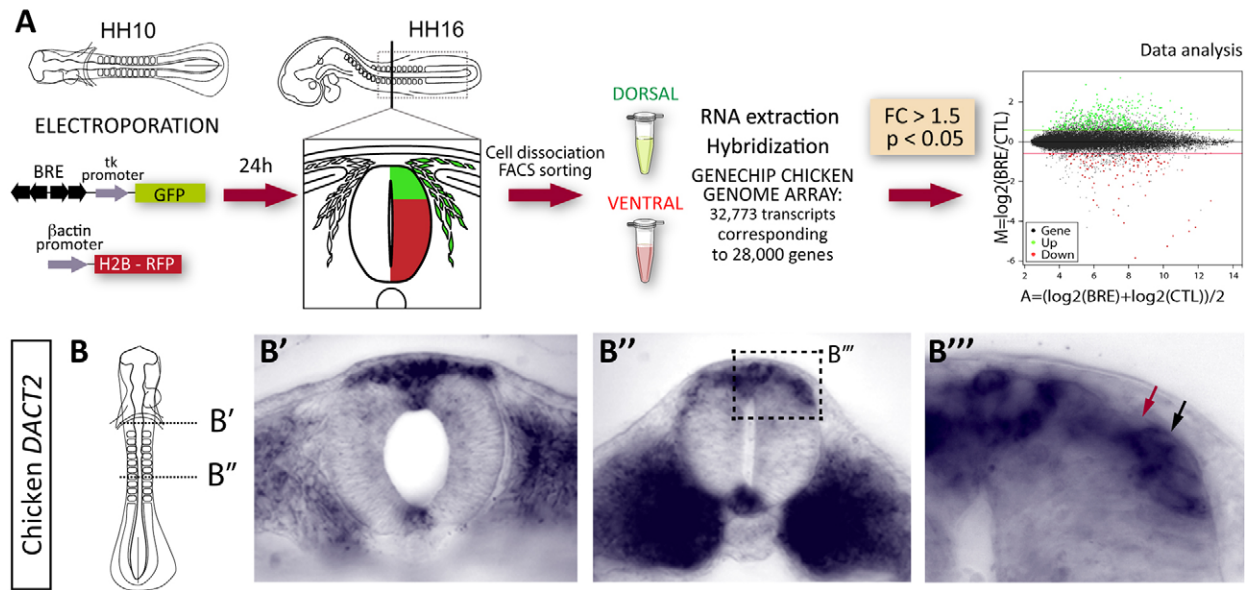
Fig. 3. DACT is expressed in neural crest cells. (A) Scheme representing chick embryos electroporated at HH10 with BRE-tk-EGFP and pCAGGS-ires-H2B-RFP, in which the transfected EGFP/RFP-expressing cells were FACS sorted 24 hpe and their RNA was extracted and hybridised to full genome Affymetrix gene chips. *Dact2* was among the genes differentially expressed in the EGFP$^+$ (dorsal) and EGFP$^-$ (ventral) cell populations (Rabadán et al., 2013). (B) Scheme of a HH10 stage chick embryo indicating the level of the sections. (B′-B″) Selected images showing *Dact2* expression in a group of cells restricted to the dorsal-most NT, early migratory NC cells and in the floor plate. (B″) Posterior section shows additional *Dact2* expression in the somites. (B‴) High magnification of inset in B″, arrows indicate *Dact2*$^+$ (black) and *Dact2*$^-$ (red) cells in the dorsal NT.

Xenopus embryo (Hikasa and Sokol, 2004; Schubert et al., 2014). Interestingly, *Dact2*-expressing cells in the dorsal NT were intermingled with *Dact2*-negative cells (Fig. 3B). Thus, since Dact1/2 exhibited a conserved expression in the premigratory NC, we set out to test whether these proteins influence NC development.

To study the role of Dact2 in chick embryos, we generated short-hairpin (sh)-RNAs specific for the chick *Dact2* sequence (Fig. S2A-D) and we found that they reduced *Dact2* expression by ∼65% (Fig. S2A-C), without affecting NC proliferation or survival (Fig. S2E,F). When the shDact2 was electroporated into HH stage 10 chick embryos, the expression of NC-specific genes, such as *FoxD3*, *Sox10* and *Snail2* was maintained and they are therefore largely independent of Dact2 activity, (Fig. S2G-V). Hence, early NC specification appears to be independent of Dact2 in the chick embryo. Knockdown of *Dact2* in chick embryos blocked NC migration in a cell-autonomous manner, with the loss of Dact2 (loss of function or LOF) leading to the retention of these cells within the NT at 24 hpe (ratio: 0.38±0.04 migratory cells). By contrast, overexpression of Dact2 (gain of function or GOF) enhanced NC migration (ratio: 1.57±0.15 migratory cells; Fig. 4A-E) and the number of GFP-labelled cells in all trunk NC derivatives increased (dorsal root ganglia, sympathetic ganglia and melanocytes; Fig. S2W,X), suggesting a common role for Dact2 in the migration of all trunk NC cells.

To study the role of Dact1 in *Xenopus* embryos, we inhibited Dact1 translation by injecting specific antisense oligo-morpholinos (MOs) into one blastomere of an eight-cell stage *Xenopus* embryo (Fig. 4F, see also Fig. S3). Injection of the Dact1-MO (LOF) reduced the extension of the cephalic NC migratory streams relative to the control uninjected side of the embryos (75% penetrance) and the size of NC derivatives was diminished (Fig. 4G-L). Conversely, overexpressing Dact1 (GOF) augmented the extension of the cephalic NC migratory streams beyond that of the control uninjected side of the embryos (60%

penetrance; Fig. 4G-L). Together, these observations indicated a conserved role for Dact1/2 in NC development, although it was not possible to distinguish between impaired delamination and/or impaired migration of NC cells.

Activity of Dact1/2 is dispensable for NC cell motility

The influence of Dact1/2 on the motility of NC cells was analysed directly using a chick neural tube explant assay and following cell movement by time-lapse microscopy (Fig. 5A; see Materials and Methods). Silencing of *Dact2* provoked the retention of NC cells within the NT, impeding analysis of their motility. However, analysis of NC cells leaving the NT explants from control and Dact2-overexpressing embryos, showed these cells migrating with similar persistence (Fig. 5B-E, Movie 1). However, there was a small but significant increase in the speed of migration when Dact2 was overexpressed (control, 1.5±0.07 mm/min; GOF, 1.7±0.06 mm/min; Fig. 4D); these cells delaminated more rapidly from the explant than control cells. As such, 50% of the Dact2-overexpressing cells had covered the first 25 μm in about 40 min, whereas the control cells required ∼55 min to achieve such release (Fig. 4C). This difference was maintained over longer distances (Fig. S4A-C). Because this small increase in speed was not sufficient to explain the differences in the distances travelled, these results suggested that Dact2 overexpression enhanced the capacity of NC cells to delaminate from the dorsal NT.

We also tested the motility of NC cells in a *Xenopus* explant assay. In *Xenopus*, cephalic NC cells start their migration as a cohesive cell population before progressively dissociating and migrating as individual cells (Carmona-Fontaine et al., 2011). Thus, NC clusters were obtained from control, Dact1-MO (LOF) and *dact1*-injected embryos (GOF), and cell motility was measured *in vitro* by time-lapse microscopy (Fig. 5F). These NC cells spread radially with similar persistence and speed, irrespective of the loss or gain of Dact1 activity and without
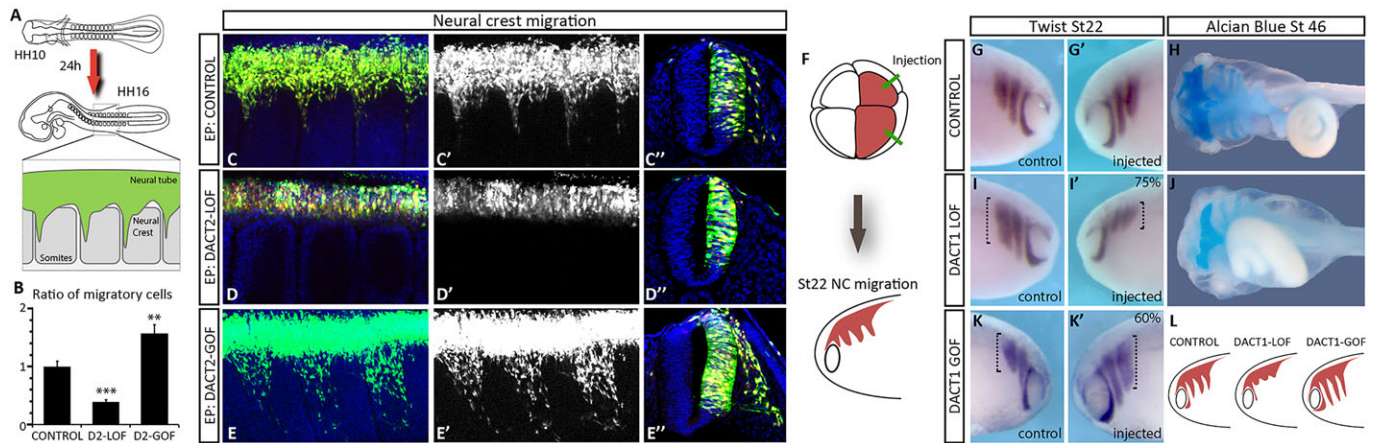
Fig. 4. Dact1/2 activity regulates NC delamination. (A) Scheme of chick embryos electroporated at HH10 in which the location of the transfected cells was analysed (reporter GFP expression). (B) Quantification of the ratio (±s.e.m.) of EGFP-expressing cells in control, shDact2 (D2-LOF) and *Dact2* (D2-GOF) electroporated embryos (*n*=10-20 sections from ≥4 embryos/condition; **P<0.01, ***P<0.001, one-way ANOVA). (C-E) Selected images of embryos electroporated at HH10 with the DNAs indicated in which the migration of the GFP-expressing cells was analysed 24 hpe in a whole-mount preparation. Lateral view shows NC streams over 3 somites of the embryos. (C″,D″,E″) Selected transverse sections of electroporated NTs showing migratory NC cells (green) in the three conditions. DAPI (blue) shows nuclear staining. (F) Scheme representing *Xenopus* embryos injected at the eight cell stage and allowed to develop until the initiation of cephalic NC migration. (G-K) *Xenopus laevis* embryos injected with control, *dact1* MO (LOF) or *dact1* RNA (GOF) were fixed at stage 22. *In situ* hybridisation for *Xenopus twist1* highlights the migratory cephalic NC streams that are shorter in (75%) *dact1* LOF embryos (brackets in I,I′) and longer in (60%) *dact1* GOF embryos (brackets in K,K′). (H,J) Alcian Blue staining performed at a later stage (St46) showing that cartilage derivatives are smaller. (L) Scheme summarising the effects on the NC migratory streams (*n*≥10/15 embryos/condition).

displaying directional migration (Fig. 5G-K; see also Movie 2). Hence, the motility of these NC cells appears to be independent of DACT, predicting a role for DACT in NC delamination. To test this hypothesis we used a method to calculate cell dispersion that is independent of the size of the explant (Carmona-Fontaine et al., 2011). First, for each cell we determined its two closest neighbours using a Delaunay triangulation algorithm (see Materials and Methods) and subsequently, we measured the area of the triangle they formed, a parameter that is proportional to cell dispersion (Fig. 5G-I). These results showed that the loss of Dact1 reduced the dispersion of NC clusters [control, 5.19±1.50; Dact1-MO, 4.65±1.22 log (area) μm^2; Fig. 5L], suggesting that it is cell delamination rather than cell motility that is dependent on DACT activity. Together, these results indicate that Dact1/2 play a conserved role in NC delamination, without affecting the identity or the motility of NC cells.

Dact1/2 inhibit Wnt/β-catenin signalling and force the release of NC cells

DACT proteins were first discovered by virtue of their binding to Dishevelled, a central element in Wnt signalling (Cheyette et al., 2002; Gloy et al., 2002). Since Dact1/2 proteins interact with the Wnt pathway, we assessed whether Dact1/2 might participate in the inhibition of Wnt signalling required for NC delamination. Co-electroporation of the Top-FLASH-Luciferase reporter with either mammalian *Dact1/2* or with *Xenopus dact1*, highlighted a potent and conserved capacity to inhibit the canonical Wnt pathway Fig. S5A,B), in addition to the previously reported role in regulating Wnt and planar cell polarity (PCP) signalling (Fig. S5D) (Wen et al., 2010; Kivimäe et al., 2011). Moreover, this inhibitory property was specific to Wnt signalling, because the BMP-response element was not regulated by either *Dact1* or *Dact2* (Fig. S5C).

To identify how DACT might inhibit the canonical Wnt pathway, we set out to define how DACT interacts with Wnt signalling proteins. The Top-FLASH-luciferase reporter assay showed that Dact2 inhibits the activation of this pathway through either the

Wnt3a ligand or the stabilised form of β-catenin, yet not through a chimeric *Tcf3* transcriptional activator with the HMG box DNA-binding domain fused to the VP16 transactivator domain (*Tcf3-VP16*; Fig. 6A). Conversely, inhibition of endogenous Dact2 strongly activated the Wnt pathway (Fig. 6B) and significantly, it was capable of overcoming Wnt inhibition at the receptor level that was provoked by the expression of a dominant negative form of the Lrp6 co-receptor (*Lrp6^{DN}*). By contrast, the inhibition of Wnt transcriptional activity mediated by Tcf3 fused to the repressor domain of Engrailed (Tcf3-EnR) could not be rescued by DACT loss of function (Fig. 6B). In conjunction, these data indicate that inhibition of Dact2 occurs upstream of Tcf3 transcriptional activity.

To study how Dact2 influences NC delamination through the regulation of Wnt signalling, the Wnt pathway was activated by electroporation of a stable form of β-catenin that significantly impaired NC delamination 24 hpe (ratio: 0.47±0.05 migratory cells). This phenotype was rescued by the co-electroporation of *Dact2* (ratio: 0.79±0.09 migratory cells), although Dact2 could not rescue the loss of NC migration provoked by electroporation of *Tcf3-VP16* (ratio: 0.76±0.08 migratory cells in Tcf3-VP16 and 0.76±1.6 migratory cells in Tcf3-VP16+Dact2; Fig. 6C-G,M). Together, these results indicate that Dact2 inhibition occurs upstream of TCF-mediated transcriptional activity and it is required for NC cells to delaminate from the dorsal NT.

Electroporation of the mutant *Lrp6^{DN}* receptor enhanced NC delamination 24 hpe (ratio: 2.65±0.37 migratory cells), although this excessive delamination of NC cells was reverted by silencing endogenous Dact2 (ratio: 0.50±0.1 migratory cells). Similarly, inhibiting the Wnt pathway at the transcriptional level through the transfection of *Tcf3-EnR* also increased NC delamination (ratio: 1.51±0.12 migratory cells), yet this increase in delamination was not reverted by dampening Dact2 activity (ratio: 1.38±0.18 migratory cells; Fig. 6H-L,N). Together, these experiments indicate that delamination of NC cells requires the inhibition of canonical Wnt activity, implicating Dact2 as a potential endogenous local inhibitor.
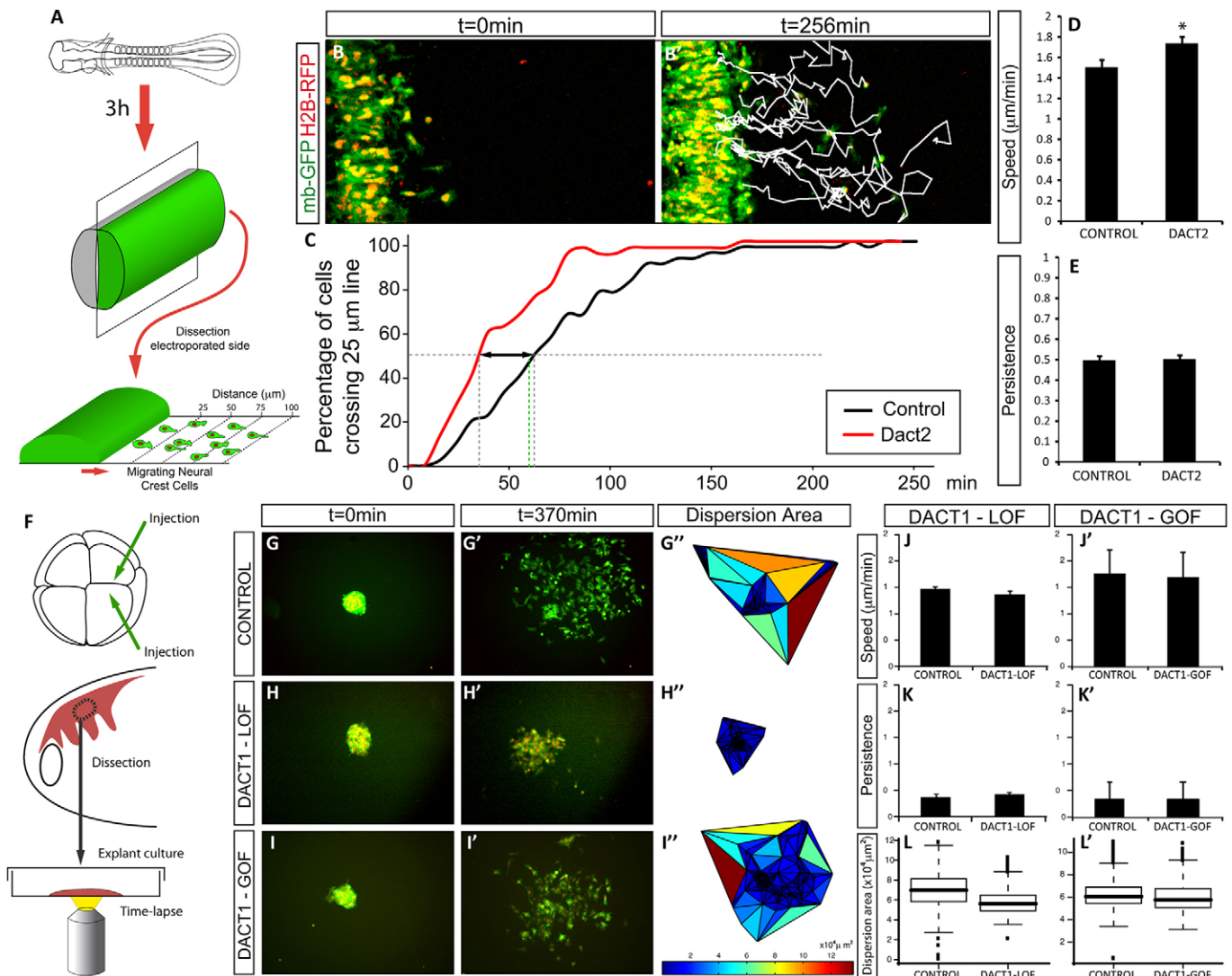
Fig. 5. DACT activity is dispensable for NC cell motility. (A) Scheme representing the explant culture and time-lapse assay for chick embryo NTs electroporated at HH10 in which the cell distance from the source (explanted NT) was analysed at 25, 50, 75 and 100 µm. (B) Selected images showing *Dact2* GOF explants at the beginning (t0) and end (t256) of the culture. (C) The plot shows the percentages of cells that cross defined points at 25 µm from the NT. (D) NC cells overexpressing *Dact2* migrate slightly faster. (E) The persistence of both cell types was identical [mean±s.e.m., $n{\geq}100$ cells of ${\geq}3$ explants/condition; *$P{<}0.05$, unpaired *t*-test (two-sided); see also Movie 1]. (F) Scheme representing the explant culture and time-lapse assay for *Xenopus laevis* embryos injected at the eight cell stage. (G-I) Selected images of control, *dact1* MO (LOF) or *dact1* mRNA expressing (GOF) explants at the beginning (t0) and end (t370) of the culture. (G″,H″,I″) Delaunay triangulations of NC explants show the more restricted dispersion in *dact1* LOF compared with the control MO explants, reflected by the reduced area between the neighbours. (J,K) The speed and persistence of both cell types is identical. (L) Dispersion is impaired in *Dact1* LOF explants (mean±s.e.m.; $n{\geq}100$ cells from ${\geq}3$ explants/condition; see also Movie 2).

The delamination of NC cells from the NT requires the disruption of the apical junctional complexes, evident as gaps in expression of N-cadherin that can be seen along the most dorsal NT from where the NC cells emigrate (Fig. S5E). Overexpression of Dact2 was insufficient to generate ectopic disruptions of junctional complexes, as seen by the integrity of N-cadherin expression at the apical pole (Fig. S5E), indicating that the structural role of β-catenin was largely resistant to Dact2 activity. These data provide further evidence that DACT specifically inhibits the transcriptional activity of β-catenin.

Dact1/2 inhibit canonical Wnt signalling by regulating the subcellular distribution of β-catenin

To search for the mechanism by which DACT proteins inhibit Wnt/β-catenin transcriptional activity, we first tested the stability of the β-catenin protein in the presence of Dact2. Fractionation of HEK-293

cells transfected with *Dact2* and β-catenin, showed that both the cytosolic and plasma membrane fraction (soluble), and the nuclear fraction (insoluble), contained full-length β-catenin, both in the presence and absence of Dact2, indicating that the stability of β-catenin was not affected by Dact2 (Fig. 7A). However, the amount of β-catenin efficiently translocated into the insoluble cell fraction was significantly higher in the presence of Dact2 (Fig. 7A,B). Confocal microscopy confirmed that Dact2 affects the subcellular localisation of β-catenin, ensuring its efficient translocation into the nucleus (Fig. 7C,D). Interestingly, β-catenin has been shown to interact directly with the three murine DACT paralogues (Kivimäe et al., 2011; Wang et al., 2015) and our data showed that a GFP-tagged version of Dact2 (Dact2-GFP) and β-catenin colocalised in spherical intranuclear punctuate structures resembling nuclear bodies (Fig. 7C,D).
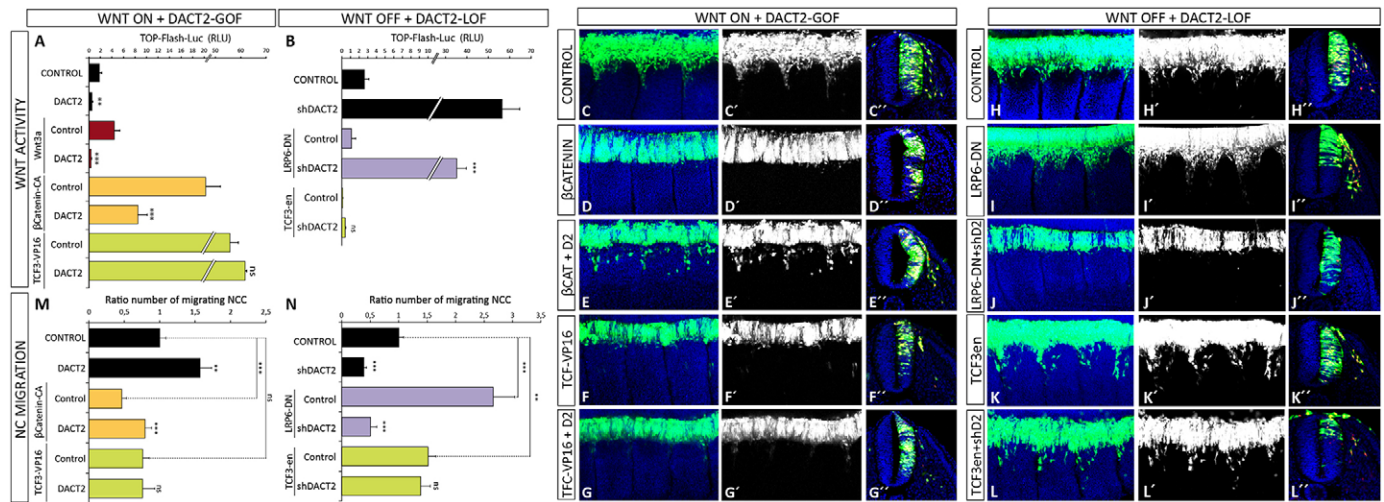
Fig. 6. DACT inhibits Wnt/β-catenin activity and forces NC cell delamination. (A) Quantification of the Luc/*Renilla* activity 24 hpe with the DNAs indicated. Dact2 inhibits the TOP-Flash reporter in control conditions and after activation by Wnt3A or CA-β-catenin, yet not after inhibition by Tcf3-VP16. (B) Converse experiments show that the shDact2 activates the TOP-Flash reporter in control conditions and after inhibition by Lrp6DN, yet not after inhibition by Tcf3-EnR (plots show mean±s.e.m., *n*=6-10 embryos/condition; ***P<0.001, one-way ANOVA). (C-L) Selected images of embryos electroporated at HH10 with the DNAs indicated in which the migration of the GFP-expressing cells was analysed 24 hpe in whole-mount preparations. Lateral view shows the NC streams over 3 somites of the embryos. (C″-L″) Selected transverse sections thorough electroporated NTs show the migratory NC cells (green) in each condition. DAPI (blue) shows nuclear staining. (M,N) Quantification of the EGFP-expressing cells after the indicated electroporations (mean±s.e.m., *n*=10-20 sections of ≥4 embryos/condition; *P<0.05, **P<0.01, ***P<0.001, one-way ANOVA).

Similarly, when we assessed the subcellular localisation of β-catenin in neuroepithelial cells from the NT of chick embryos electroporated with *Dact2* and β-catenin, the latter was efficiently translocated into the insoluble cell fraction in the presence of Dact2 (Fig. 7E,F). Interestingly, we show that a novel slower-migrating form of β-catenin appeared in the insoluble fraction, both in HEK and neuroepithelial cells, the molecular masses of which were compatible with their post-translational modification by the small ubiquitin-like modifier (SUMO, 12 kDa; Matic et al., 2010; Müller et al., 1998). Indeed, the slower-migrating forms of β-catenin were detected with an anti-Sumo1 antibody (Fig. 7G), indicating that a fraction of the β-catenin sequestered into nuclear bodies (NBs) is susceptible to SUMOylation. Sequence analysis identifies three highly conserved lysines (K19, K312 and K666) in β-catenin situated in inverted SUMOylation consensus motifs E/DxKψ (Matic et al., 2010), which are potential SUMO acceptors (Fig. S6A,B). Although this post-translational modification of β-catenin might be relevant for its maintenance within NBs, forced SUMOylation of β-catenin induced by co-transfection of Sumo-1 was not sufficient to either promote the translocation of β-catenin into NBs (Fig. S6C) or to reduce β-catenin-mediated transcriptional activation (Fig. S6D).

In the developing NT, endogenous β-catenin accumulated at the membrane of neuroepithelial cells, as well as apical junctional complexes (Fig. 7H,I). Although transcriptional activity requires the nuclear translocation of β-catenin, this might be a rather dynamic event as the nuclear accumulation of endogenous β-catenin in dorsal neuroepithelial cells is hardly visible (Fig. 7I). Rather, we observed an intranuclear punctuate distribution of endogenous β-catenin in dorsal NT cells that contrasted with the nuclear staining evident in migratory NC cells and the lack of β-catenin staining in non-neural ectoderm cells (Fig. 7I). To confirm that the intranuclear punctuate distribution of β-catenin was dependent on the scaffold activity of Dact1/2 proteins, we co-electroporated low levels of β-catenin that adopt the membrane localisation of the endogenous protein (as evident by confocal microscopy), together with a plasmid encoding

Dact2 fused to the enhanced green fluorescent protein (Dact2-GFP; Fig. 7J,K). Interestingly, in the presence of Dact2, β-catenin accumulates in structures resembling NBs, which also contained Dact2-GFP (Fig. 7L). Together, these data indicate that the scaffold protein Dact2 binds to and translocates β-catenin into the nucleus, where its accumulation in NBs prevents β-catenin from acting as a TCF transcriptional co-activator.

DISCUSSION

We show here that canonical Wnt/β-catenin activity must be inhibited in order for NC cells to complete EMT and delaminate from the dorsal NT. Moreover, we show that this inhibition of the Wnt pathway occurs in a cell-autonomous manner and that it is dependent on the activity of the scaffold proteins Dact1/2. In searching for the mechanism that mediates β-catenin inhibition, we found that DACT proteins control the subcellular distribution of β-catenin, preventing it from mediating transcriptional responses. This is a reversible inhibitory mechanism and indeed, NC cells that have migrated away from the neural tube reactivate the Wnt pathway.

Reversible inhibition of Wnt/β-catenin activity

The DACT family of scaffold proteins was discovered by virtue of binding to Dvl proteins central to Wnt/PCP signalling (Gloy, et al., 2002; Cheyette, et al., 2002). More recent data showed that these scaffold proteins can form complexes with β-catenin (Cheyette et al., 2002; Gao et al., 2008; Kivimäe et al., 2011; Wang et al., 2015), which is a key mediator of the Wnt signalling pathway (Clevers and Nusse, 2012). Although we do not rule out a contribution of DACT in non-canonical Wnt signalling, as previously shown in *Xenopus* embryos (Park et al., 2006; Wen et al., 2010; Kivimäe et al., 2011), our results show a strong and conserved inhibitory role played by DACT proteins in the canonical Wnt pathway. In the presence of Dact1/2, we show here that β-catenin was efficiently translocated to the insoluble cell fraction and it accumulated in spherical intranuclear structures that resemble
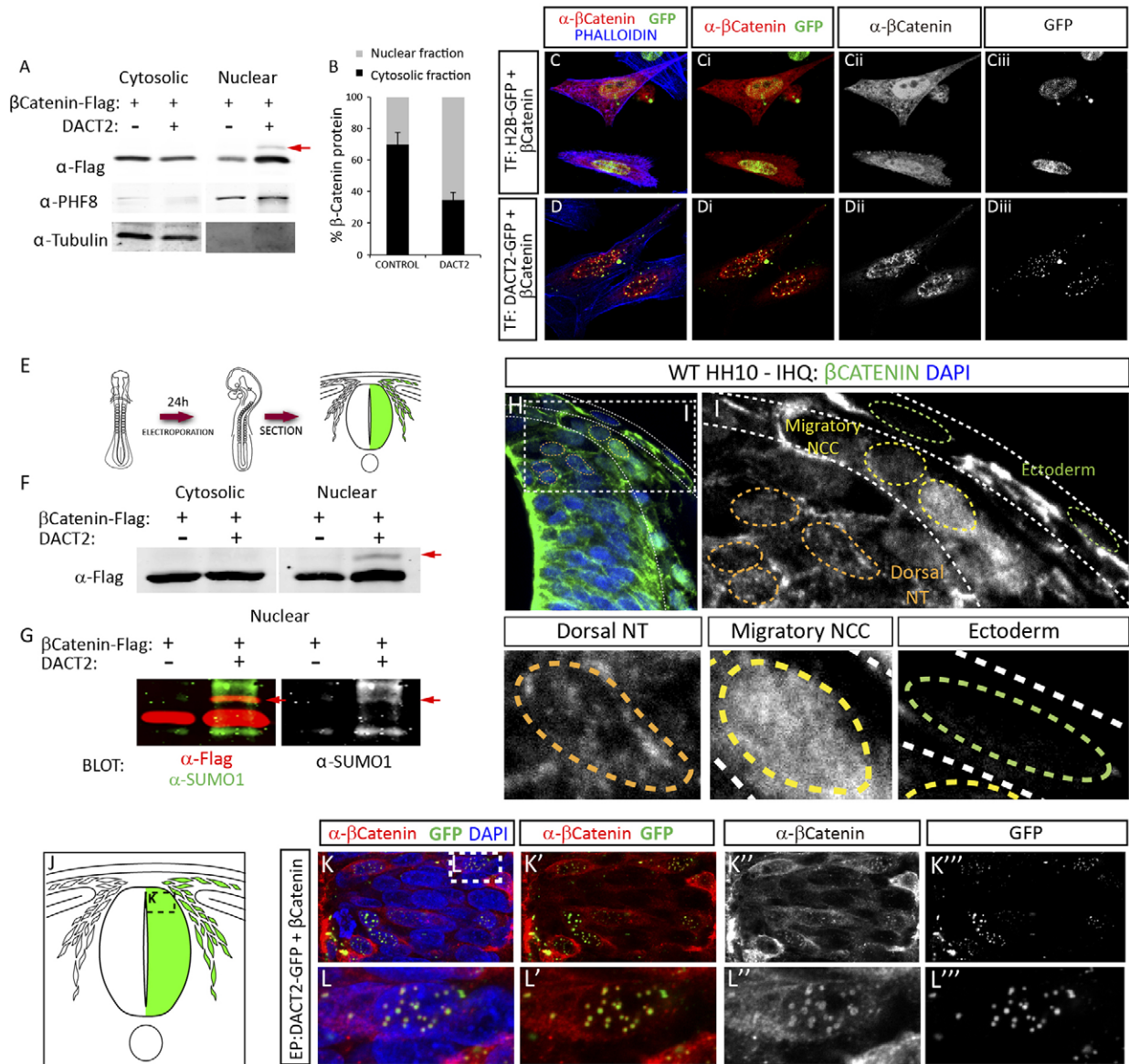
Fig. 7. Dact2 mediates β-catenin segregation into nuclear bodies. (A) HEK-293 cells were transfected with the DNAs indicated, and the NP40-soluble and -insoluble fractions were analysed in western blots probed with antibodies against Flag (for β-catenin detection), PHF8 (control for the nuclear cell fraction) and α-tubulin (control for the cytosolic cell fraction). Dact2 induced the accumulation of β-catenin in the insoluble nuclear fraction, where a novel slow-migrating band of β-catenin appeared (red arrow). (B) Quantification of protein expression in the indicated cell fractions. (C,D) Selected images of HEK-293 cells transfected with the DNAs indicated. (C-C‴) In control transfections, β-catenin (red) was localised throughout the cell (cytoplasm+nucleus). (D-D‴) In the presence of DACT2: GFP, β-catenin (red) accumulated in NBs, where it colocalises with DACT2 (green). (E) Scheme representing the chick embryos electroporated at HH10 that were analysed 24 hpe in western blots. (F) The cytosolic and nuclear fractions were probed with antibodies against Flag. Dact2 induced the accumulation of β-catenin in the nuclear fraction where a novel slow-migrating band of β-catenin appeared (red arrow). (G) When probed with antibody against SUMO1, the slow-migrating band of β-catenin was SUMOylated (arrow). (H,I) Selected images of the subcellular distribution of endogenous β-catenin (green) in a wild-type stage HH12 chick embryo. DAPI (blue) shows nuclear staining. (I) Neuroepithelial cells in the dorsal NT show nuclear punctuate accumulations of β-catenin, which do not appear in the nucleus of migratory NC cells. No nuclear β-catenin is evident in non-neural ectodermal cells. (J) Scheme representing the chick embryos electroporated at HH10 with the DNAs indicated and immunostained for β-catenin (K) The subcellular distribution of EP-β-catenin resembles the wild-type distribution at the membrane. (L) In cells co-expressing Dact2 (green), β-catenin accumulates in NBs that also contain Dact2. DAPI (blue) shows nuclear staining.

NBs. NBs compartmentalise the nuclear environment, regulating activities such as gene transcription and many resident NB proteins suffer modifications that reinforce these associations (Mao et al., 2011). Interestingly, we describe a novel slower-migrating form of β-catenin whose molecular mass was compatible with post-translational modification by SUMO (12 kDa; Matic et al., 2010; Müller et al., 1998). Sequence analysis identifies three highly conserved lysines (K19, K312 and K666) in β-catenin that are situated in inverted SUMOylation E/DxKψ consensus motifs

(Matic et al., 2010) as potential SUMO acceptors. Although this post-translational modification of β-catenin might be relevant for its maintenance within NBs, forced SUMOylation of β-catenin was not sufficient to either promote the translocation of β-catenin into NBs or to reduce β-catenin-mediated transcriptional activation. This additional data reinforces our model whereby the Dact1/2 scaffold proteins expressed in the dorsal NT control the subcellular distribution of β-catenin, transiently preventing transcriptional responses.

The localisation of β-catenin to NBs has been observed in tumour cells (Satow et al., 2012; Zhang et al., 2014), where a direct interaction between the armadillo repeat of β-catenin and the product of promyelocytic leukaemia (PML) protein was reported (Satow et al., 2012). Among the different NBs, not only the PML NBs but also the polycomb group (PcG) NBs act as SUMOylation centres and hubs for gene repression. The canonical Wnt pathway can be regulated by SUMOylation, particularly in terms of TCF/LEF-mediated transcription (Sachdev et al., 2001; Yamamoto et al., 2003). Unlike ubiquitylation, which targets proteins for degradation, SUMOylation is a reversible post-translational modification that can be reversed by SUMO-specific proteases (SENPs). This might be the case for β-catenin once NC cells have completed the EMT and delaminated from the dorsal neural tube, because we show that a subset of migratory NC cells reactivate the Wnt/β-catenin pathway.

Multiple Wnt activities in neural crest development

NC development requires the intervention of Wnt activity at multiple stages, from the initial induction of NC identity to their migration and ultimate lineage decisions. Initially, the acquisition of NC identity is mediated by Wnt activation and BMP inhibition during the early gastrula stages, which is later maintained by both BMP and Wnt activation from tissues adjacent to the NC (García-Castro et al., 2002; Steventon et al., 2009; De Calisto et al., 2005; Carmona-Fontaine et al., 2008). As such a direct target of Wnt activity, Gbx2 is required for NC specification (Li et al., 2009). However, we show that the expression of NC genes such as *FoxD3* or *Sox10* is refractory to the regulation of Wnt activity at later stages. Moreover, the expression of Snail, the main effector of the EMT implicated in NC delamination, is directly activated by Wnt activity (Ten Berge et al., 2008). However, our results show that activation of β-catenin-mediated transcriptional responses by injection of a *dact1* MO into two-cell stage *Xenopus* embryos, or by electroporation of shDact2 into HH stage 10 chick embryos, diminished *Snail2* expression, which opposes the β-catenin activation of *Snail2* expression and favours EMT. Together, these data indicate the regulation of an as yet unknown β-catenin transcriptional target that inhibits neural crest delamination.

The migratory properties of NC cells appear to be mainly regulated by non-canonical Wnt signalling (De Calisto et al., 2005; Carmona-Fontaine et al., 2008; Matthews et al., 2008; Mayor and Theveneau, 2014). Indeed, NC cells appear to spread without displaying directional migration, with similar penetrance and speed of migration irrespective of the activity of the Wnt pathway. Thus, our results confirm that the motility of NC cells is largely independent of canonical Wnt activity and accordingly, these properties are not regulated by DACT.

Finally, lineage specification and the differentiation of NC derivatives also appear to depend on the Wnt/β-catenin pathway. Derivatives of the trunk NC include those cells that migrate through the ventral pathway to populate both the sensory and sympathetic ganglia, and those that follow the dorsolateral pathway to become melanocytes. Constitutive activation of β-catenin in NC explants from mouse embryos appears to promote sensory neurogenesis (Lee et al., 2004), whereas activation of β-catenin in migratory NC cells promotes the generation of melanocytes (Hari et al., 2012). Here, we show that Dact2 promotes the migration of all trunk NC-derived cells, regardless of their identity. In conclusion, we show that the inhibitory effect of Dact2 on β-catenin is required during a very short and precise time window associated with EMT and that it is required for the delamination of all trunk NC lineages.

MATERIALS AND METHODS
Chick and *Xenopus* embryo manipulation
Fertilised eggs from female *Xenopus laevis* were injected with 5-10 nl RNA (50 ng/ml) or morpholino probes (800 ng/ml) with 5% Ficoll in 75% NAM, along with FLDx (Molecular Probes), and they were maintained in this medium until stage 6-8. All injections to target the NC were performed in the lateral animal blastomeres at the 4- to 8-cell stage. Embryos were incubated at 14.5°C and staged according to Niewkoop and Faber (1994). Animal cap assays were carried out as described elsewhere (De Calisto et al., 2005) and the cartilage in *Xenopus* tadpoles was stained with Alcian Blue following standard procedures.

Eggs from white Leghorn chickens were incubated at 38.5°C in an atmosphere of 70% humidity, and the embryos were staged according to Hamburger and Hamilton (1951). Chick embryos were electroporated with Clontech purified plasmid DNA (2-3 μg/ml in H$_2$O) with Fast Green (50 ng/ml). Briefly, plasmid DNA was injected into the lumen of the NT and electrodes were placed either side of the embryo to perform electroporation using an Intracel Dual Pulse (TSS10) electroporator, delivering five 50 ms pulses of 20-30 V.

Fluorescence-associated cell sorting (FACS) and microarray analysis
Plasmid DNA encoding the pBRE-tk-EGFP reporter construct and the pCAGGS-IRES-H2B-RFP construct were co-electroporated into chick embryos and the NT was dissected out of the embryos 24 h later. Thirty electroporated embryos were pooled and a single-cell suspension was obtained following 10-15 min incubation with trypsin-EDTA (Sigma), and GFP and RFP fluorescent cells were sorted using a MoFlo flow cytometer (DakoCytomation). At least 100,000 RFP$^+$ cells and 20,000 GFP$^+$ cells were obtained per pool, and total RNA was extracted from the resulting cell sorted populations (∼90% of RFP$^+$/GFP$^+$ cells or 90% of RFP$^+$/GFP$^-$ cells), using a standard Trizol (Promega) protocol. The quality and quantity of purified RNA was verified by measuring with Nanodrop, and subsequently the RNA was hybridised to microarrays and the arrays processed in accordance to the manufacturer's instructions (Affymetrix). Two-cycle cDNA synthesis was performed on 35-50 ng total RNA and hybridised to the GeneChip Chicken Genome Array (Affymetrix) (Rabadán et al., 2013). For statistical analysis, the data from four biological replicates of each experiment were averaged and microarray data was analysed using Bioconductor software. The quality of the data was assessed, normalised with the 'rma' algorithm and differentially expressed genes were selected. The results were filtered using thresholds of [log2FC]>0.5849 and *P*<0.05.

DNA constructs
The BMP reporter construct (BRE-tk-GFP; Le Dréau et al., 2012), the Wnt reporter TOP-FLASH-Luciferase (Korinek et al., 1998) and TOP-FLASH-2dEGFP constructs (Rios et al., 2010) were as published. The following DNAs were inserted into pCIG: full-length mouse *Wnt3a* coding sequence; a mutant S33Y form of β-catenin; the HMG box of *Tcf3* fused to VP16 or to the engrailed-repressor enR; and a mutant *Lrp6* that acts as a dominant-negative co-receptor (Alvarez-Medina et al., 2009). Human *DACT1* and *DACT2* constructs were a generous gift from Dr N. B. Cheyette (UCSF, USA). The β-catenin construct fused to Flag and the *Dact2* construct fused to GFP were cloned into pCIEGO. The pcDNA3.1-human SUMO1-HA was a generous gift from Manuel Rodriguez (de la Cruz-Herrera et al., 2015) and the cDNAs encoding Dact1 (Gloy et al., 2002), Fz7, Dsh-GFP and membrane-Cherry were all cloned into pCS2 and used for RNA synthesis.

For *in vivo* LOF experiments in *Xenopus* embryos, the 24-mer *dact1* MO used to prevent *dact1* mRNA translation was as published (Gloy et al., 2002): 5′-TGGGCTTCATCCTGGGACAGCGA-3′ (from GeneTools, Philomath, OR). The control morpholino had the following sequence; 5′-AGAGACTTGATACAGATTCGAGAAT-3′.

For *in vivo* loss-of-function (LOF) experiments in chick embryos, short hairpin-based expression vectors for RNAi were generated using the

pSUPER RNAi system (OligoEngine). A pair of custom oligonucleotides that contained a unique 19 nt sequence derived from chicken *Dact2* mRNA were designed using the RNAi Design Tool (www.oligoengine.com). Forward and reverse 64 nt oligos (Sigma) were used for annealing and cloning into the pSUPER vector, according to the manufacturer's guidelines. The sequences used were: DACT 2.1 FOR, 5′-GATCCCCGA-CAGTGAGTCCAGTGAAATTCAAGAGATTTCACTGGACTCACTGT-CTTTTTA-3′; REV, 5′-AGCTTAAAAAGACAGTGAGTCCAGTGAA-ATCTCTTGAATTTCACTGGACTCACTGTCGGG-3′; DACT 2.2 FOR, 5′-GATCCCCGCATTGATGTGTACCCTTATTCAAGAGATAAGGG-TACACATCAATGCTTTTTA-3′; REV, 5′-AGCTTAAAAAGCATTG-ATGTGTACCCTTATCTCTTGAATAAGGGTACACATCAATGCGG-G-3′; DACT 2.3 FOR, 5′-GATCCCCGGGCTACATCAATAAATTAT-TCAAGAGATAAATTTATTGATGTAGCCCTTTTTGGAAA-3′; REV, 5′-AGCTTTTCCAAAAAGGGCTACATCAATAAATTATCTCTTGAAT-AATTTATTGATGTAGCCCGGG-3′.

To quantify the loss of DACT expression at a cell-autonomous level, a fragment of chick *Dact2* containing the target sequence of shDact2 was cloned into H2B-RFP pCIG and co-electroporated with a constitutive GFP expression vector. Levels of RFP expression were measured in the GFP expressing areas using ImageJ (NIH) software. A control shRNA was generated against the human *HDAC* sequence, cloned into the pSUPER vector and electroporated at the same developmental stages as a control for each experiment.

RT-quantitative real-time PCR
Plasmids encoding EGFP were electroporated into embryos and their neural tubes were dissected at 24-48 hpe. Single-cell suspensions were obtained following a 10-15 min digestion with trypsin-EDTA (Sigma) and GFP-expressing cells were FACS sorted, extracting the total RNA from the resulting cell populations. Real-time RT-PCR reactions were carried out in triplicate using fixed amounts of template DNA, SYBR green detection and oligonucleotide primers from Qiagen (cSnail2, QT00642376; cFoxD3, QT00592655; cFoxD3, QT01482670; cSox10, QT00591521; cDact2, QT00645491; QuantiTec Primer Assays). GAPDH (Fw: cctctctggcaaagtc-caag, Rv: catctgcccatttgatgttg) and β-actin (Fw: gatgaagcccagagcaaaag, Rv: ggggtgttgaaggtctcaaa) were amplified as controls. Standard curves were obtained for each amplicon by plotting the number of cycles at which the fluorescence crossed the threshold (crossing values) against increasing amounts of DNA template. All experimental values were normalised to those obtained for GAPDH and PCR amplifications were assessed from four independent cell pools for each experimental condition. The data are expressed in arbitrary units and represent mean standardised values±s.e.m.

In situ hybridisation in chick and *Xenopus* embryos
For *in situ* hybridisation, chick embryos were fixed overnight at 4°C in 4% paraformaldehyde (PFA) in PBS, after which they were rinsed and processed for whole-mount RNA *in situ* hybridisation following standard procedures. The embryos were hybridised with probes against chick *Dact2*, *FoxD3*, *Sox10* and *Snail2* (from the chicken EST project, UK-HGMP RC), the binding of which was visualised with alkaline phosphatase-coupled anti-digoxigenin Fab fragments (Boehringer Mannheim). Hybridised embryos were post-fixed in 4% PFA, rinsed in PBT (PBS with 0.1% Triton) and vibratome sections were analysed.

In situ hybridisation was performed in *Xenopus* embryos following standard procedures, using probes for *Xenopus dact1* (Gloy et al., 2002), *sox2* (Gloy et al., 2002), *snail2* (Mayor et al., 1995) and *twist1* (Hopwood et al., 1989). Representative images were obtained from at least three independent embryos per experimental condition on a Leica DMR microscope.

Immunohistochemistry
For immunohistochemistry, embryos were fixed for 2-4 h at 4°C with 4% PFA in PBS, and immunostaining was performed on either vibratome or cryostat sections following standard procedures using antibodies against the following proteins: caspase3 (C92-605, BD Pharmingen, 1:500); phospho-histone H3 (06-570, Upstate Biochemicals, 1:500); β-catenin (C7207, Sigma, 1:1000), HNK-1 (C6680, Sigma, 1:1000), AP2 (3B5

DSHB, 1:200). Alexa Fluor 555- and 633-conjugated anti-mouse or anti-rabbit secondary antibodies (Molecular Probes) were used and Phalloidin-Rhodamine (Sigma) staining was also performed. After single or dual staining, the sections were mounted, photographed on a Leica SP5 confocal microscope and processed with Adobe Photoshop CS5. Cell counting was performed on confocal images of 10-20 different sections from at least four different embryos in each experimental condition.

To quantify the Top-2dEGFP/RFP ratios of fluorescence intensity, confocal images obtained on a Zeiss LSM780 microscope were analysed using ImageJ. The nuclear area of the electroporated cells was defined by polygonal selection, and the mean grey value intensity of this area was determined for RFP and GFP. The distance of this nucleus to the reference point (intersection between the ectoderm and neural tube) was then measured, quantifying 46 different images from 8 embryos and a total of 230 cells. The results are shown as the GFP/RFP ratio and represented as a function of the distance.

Immunoblotting and subcellular fractionation
For cell fractionation, chick embryos or HEK-293 cell cultures were electroporated with β-catenin-Flag alone, or in combination of DACT2:GFP or SUMO1-HA (a gift from Dr Manuel Rodriguez, Cancer Unit, Inbiomed, Gipuzkoa, Spain). Samples were obtained 48 hpe, lysed in NP40 buffer (150 mM NaCl, 1% NP-40, 50 mM Tris-HCl, pH 7.5 and 1 mM PMSF) and centrifuged at 20,000 g for 30 min at 4°C. The resulting supernatant and pellet, considered as the NP40-soluble and -insoluble fractions, respectively, were resolved by SDS-PAGE and analysed by western blot probed with rabbit polyclonal anti-Flag (R1, produced in the lab, 1:2000), mouse monoclonal anti-human SUMO1 (Santa Cruz, sc-5308, 1:2000), mouse monoclonal anti-α-tubulin (Sigma,T6119,1:1000) or rabbit polyclonal anti-PHF8 (Abcam, 36068, 1:1000). The α-tubulin and PHF8 proteins were used as NP40-soluble and -insoluble reference proteins, respectively. All antibodies were detected with fluorescent secondary antibodies and scanned with an Odyssey Imaging System from Lycor. The expression values were quantified with Quantity One software (Bio-Rad) and they are expressed as the means±s.d. of three independent experiments.

Chick and *Xenopus* embryo NC explant cultures and time-lapse analysis
HH stage 10 chick embryos were electroporated with the DNAs indicated and the NT was dissected out at 3 hpe. NT explants were cultured in fibronectin (Sigma)-coated plastic dishes with DMEM-F12 (D6421, Sigma), 0.01% penicillin-streptomycin (Invitrogen) and 0.001% Myto[+] (BD BioScience). Time-lapse imaging of migrating NC cells was performed on a Leica SP5 confocal microscope, as described previously (Ferronha et al., 2013). Cell-tracking assays were processed using ImageJ, treating migratory cells as particles centred on their own nuclei and then tracking them with the ImageJ 'manual tracking' plug-in.

For *Xenopus* embryos, the time-lapse imaging and tracking of migrating NC cells was performed as described elsewhere (Carmona-Fontaine et al., 2008; Matthews et al., 2008). The cells injected with nuclear-RFP/membrane-GFP or membrane-RFP/nuclear-GFP were analysed by DIC or fluorescent microscopy on a DM5500 Leica compound microscope. The cells were treated as particles centred on their own nuclei and then tracked using ImageJ 'manual tracking' plug-in. Computer analysis was performed with ImageJ and using in-house scripts produced in MatLab (R14b, MathWorks).

Luciferase reporter assay
An *in vivo* assay of transcriptional activity was used to assess distinct DACT constructs and different components of the canonical Wnt pathway. Chick embryos were electroporated with the DNAs indicated or with the empty pCIG or pSHIN vectors as a control, together with the firefly luciferase vector and a *Renilla* luciferase reporter constructs carrying the CMV immediate early enhancer promoter (Promega) for normalisation. The firefly luciferase reporters used were the TOP-FLASH luciferase reporter construct containing synthetic TCF binding sites (Alvarez-Medina et al., 2009) and the BRE-Luc (Le Dréau et al., 2012). Embryos were harvested 24 h later and GFP-positive NT cells were dissected out and homogenised in passive lysis

buffer with a Dounce homogeniser on ice. Firefly luciferase and *Renilla* activities were measured using the Dual Luciferase Reporter Assay System (Promega), a Sirius Luminometer (Berthold) and FB12 Sirius software. The data are presented as the mean±s.e.m. from 11-12 embryos per experimental condition.

Quantification and statistical analysis

The quantitative data are expressed as the mean±s.e.m. Statistical analysis was performed using the Statview software and the significance of the data was assessed by performing ANOVA followed by the Student–Newman–Keuls test. Errors were estimated using the corresponding formulae for the standard error propagation technique: $*P<0.05$, $**P<0.01$ and $***P<0.001$.

References

Alvares, L. E., Winterbottom, F. L., Jorge, E. C., Rodrigues Sobreira, D., Xavier-Neto, J., Schubert, F. R. and Dietrich, S. (2009). Chicken dapper genes are versatile markers for mesodermal tissues, embryonic muscle stem cells, neural crest cells, and neurogenic placodes. *Dev. Dyn.* **238**, 1166-1178.

Alvarez-Medina, R., Le Dreau, G., Ros, M. and Marti, E. (2009). Hedgehog activation is required upstream of Wnt signalling to control neural progenitor proliferation. *Development* **136**, 3301-3309.

Betancur, P., Bronner-Fraser, M. and Sauka-Spengler, T. (2010). Assembling neural crest gene regulatory circuits into a gene regulatory network. *Annu. Rev. Cell Dev. Biol.* **26**, 581-603.

Carmona-Fontaine, C., Matthews, H. and Mayor, R. (2008). Directional cell migration in vivo: Wnt at the crest. *Cell Adh. Migr.* **2**, 240-242.

Carmona-Fontaine, C., Theveneau, E., Tzekou, A., Tada, M., Woods, M., Page, K. M., Parsons, M., Lambris, J. D. and Mayor, R. (2011). Complement fragment C3a controls mutual cell attraction during collective cell migration. *Dev. Cell* **21**, 1026-1037.

Cheyette, B. N. R., Waxman, J. S., Miller, J. R., Takemaru, K.-I., Sheldahl, L. C., Khlebtsova, N., Fox, E. P., Earnest, T. and Moon, R. T. (2002). Dapper, a Dishevelled-associated antagonist of beta-catenin and JNK signaling, is required for notochord formation. *Dev. Cell* **2**, 449-461.

Clevers, H. and Nusse, R. (2012). Wnt/β-catenin signaling and disease. *Cell* **149**, 1192-1205.

De Calisto, J., Araya, C., Marchant, L., Riaz, C. F. and Mayor, R. (2005). Essential role of non-canonical Wnt signalling in neural crest migration. *Development* **132**, 2587-2597.

De la Cruz-Herrera, C. F., Baz-Martínez, M., Lang, V., El Motiam, A., Barbazán, J., Couceiro, R., Abal, M., Vidal, A., Esteban, M., Muñoz-Fontela, C. et al. (2015). Conjugation of SUMO to p85 leads to a novel mechanism of PI3K regulation. *Oncogene*, doi: 10.1038/onc.2015.356.

Ferronha, T., Rabadan, M. A., Gil-Guiñon, E., Le Dreau, G., de Torres, C. and Marti, E. (2013). LMO4 is an essential cofactor in the snail2-mediated epithelial-to-mesenchymal transition of neuroblastoma and neural crest cells. *J. Neurosci.* **33**, 2773-2783.

Gao, X., Wen, J., Zhang, L., Li, X., Ning, Y., Meng, A. and Chen, Y.-G. (2008). Dapper1 is a nucleocytoplasmic shuttling protein that negatively modulates Wnt signaling in the nucleus. *J. Biol. Chem.* **283**, 35679-35688.

García-Castro, M. I., Marcelle, C. and Bronner-Fraser, M. (2002). Ectodermal Wnt function as a neural crest inducer. *Science* **297**, 848-851.

Gloy, J., Hikasa, H. and Sokol, S. Y. (2002). Frodo interacts with Dishevelled to transducer Wnt signals. *Nat. Cell Biol.* **4**, 351-357.

Hamburger, V. and Hamilton, H. L. (1951). A series of normal stages in the development of the chick embryo. *J. Morphol.* **88**, 49-92.

Hari, L., Miescher, I., Shakhova, O., Suter, U., Chin, L., Taketo, M., Richardson, W. D., Kessaris, N. and Sommer, L. (2012). Temporal control of neural crest lineage generation by Wnt/β-catenin signaling. *Development* **139**, 2107-2117.

Herrera, A., Saade, M., Menendez, A., Marti, E. and Pons, S. (2014). Sustained Wnt/β-catenin signalling causes neuroepithelial aberrations through the accumulation of aPKC at the apical pole. *Nat. Commun.* **9**, 4168.

Hikasa, H. and Sokol, S. Y. (2004). The involvement of Frodo in TCF-dependent signaling and neural tissue development. *Development* **131**, 4725-4734.

Hopwood, N. D., Pluck, A. and Gurdon, J. B. (1989). A Xenopus mRNA related to Drosophila twist is expressed in response to induction in the mesoderm and the neural crest. *Cell* **59**, 893-903.

Kivimäe, S., Yang, X. Y. and Cheyette, B. N. (2011). All Dact (Dapper/Frodo) scaffold proteins dimerize and exhibit conserved interactions with Vangl, Dvl, and serine/threonine kinases. *BMC Biochem.* **12**, 33.

Korinek, V., Barker, N., Willert, K., Molenaar, M., Roose, J., Wagenaar, G., Markman, M., Lamers, W., Destree, O. and Clevers, H. (1998). Two members of the Tcf family implicated in Wnt/beta-catenin signaling during embryogenesis in the mouse. *Mol. Cell. Biol.* **18**, 1248-1256.

Le Dréau, G., Garcia-Campmany, L., Rabadán, M. A., Ferronha, T., Tozer, S., Briscoe, J. and Martí, E. (2012). Canonical BMP7 activity is required for the generation of discrete neuronal populations in the dorsal spinal cord. *Development* **139**, 259-268.

Lee, H.-Y., Kléber, M., Hari, L., Brault, V., Suter, U., Taketo, M. M., Kemler, R. and Sommer, L. (2004). Instructive role of Wnt/beta-catenin in sensory fate specification in neural crest stem cells. *Science* **303**, 1020-1023.

Li, B., Kuriyama, S., Moreno, M. and Mayor, R. (2009). The posteriorizing gene Gbx2 is a direct target of Wnt signalling and the earliest factor in neural crest induction. *Development* **136**, 3267-3278.

Mao, Y. S., Zhang, B. and Spector, D. L. (2011). Biogenesis and function of nuclear bodies. *Trends Genet.* **27**, 295-306.

Matic, I., Schimmel, J., Hendriks, I. A., van Santen, M. A., van de Rijke, F., van Dam, H., Gnad, F., Mann, M. and Vertegaal, A. C. (2010). Site-specific identification of SUMO-2 targets in cells reveals an inverted SUMOylation motif and a hydrophobic cluster SUMOylation motif. *Mol. Cell* **39**, 641-652.

Matthews, H. K., Marchant, L., Carmona-Fontaine, C., Kuriyama, S., Larraín, J., Holt, M. R., Parsons, M. and Mayor, R. (2008). Directional migration of neural crest cells in vivo is regulated by Syndecan-4/Rac1 and non-canonical Wnt signaling/RhoA. *Development* **135**, 1771-1780.

Mayor, R. and Theveneau, E. (2013). The neural crest. *Development* **140**, 2247-2251.

Mayor, R. and Theveneau, E. (2014). The role of the non-canonical Wnt-planar cell polarity pathway in neural crest migration. *Biochem. J.* **457**, 19-26.

Mayor, R., Morgan, R. and Sargent, MG. (1995). Induction of the prospective neural crest of Xenopus. *Development* **121**, 767-777.

Müller, S., Matunis, M. J. and Dejean, A. (1998). Conjugation with the ubiquitin-related modifier SUMO-1 regulates the partitioning of PML within the nucleus. *EMBO J.* **17**, 61-70.

Nieto, M. A. (2013). Epithelial plasticity: a common theme in embryonic and cancer cells. *Science* **342**, 1234850.

Nieuwkoop, D., and Faber, J. (1994). *Normal Table of Xenopus laevis (Daudin)*. New York: Garland Publishing.

Park, J.-I., Ji, H., Jun, S., Gu, D., Hikasa, H., Li, L., Sokol, S. Y. and McCrea, P. D. (2006). Frodo links Dishevelled to the p120-catenin/Kaiso pathway: distinct catenin subfamilies promote Wnt signals. *Dev. Cell* **11**, 683-695.

Rabadán, M. A., Usieto, S., Lavarino, C. and Martí, E. (2013). Identification of a putative transcriptome signature common to neuroblastoma and neural crest cells. *Dev. Neurobiol.* **73**, 815-827.

Rios, A. C., Denans, N. and Marcelle, C. (2010). Real-time observation of Wnt beta-catenin signaling in the chick embryo. *Dev. Dyn.* **239**, 346-353.

Sachdev, S., Bruhn, L., Sieber, H., Pichler, A., Melchior, F. and Grosschedl, R. (2001). PIASy, a nuclear matrix-associated SUMO E3 ligase, represses LEF1 activity by sequestration into nuclear bodies. *Genes Dev.* **15**, 3088-3103.

Satow, R., Shitashige, M., Jigami, T., Fukami, K., Honda, K., Kitabayashi, I. and Yamada, T. (2012). β-catenin inhibits promyelocytic leukemia protein tumor suppressor function in colorectal cancer cells. *Gastroenterology* **142**, 572-581.

Schubert, F. R., Sobreira, D. R., Janousek, R. G., Alvares, L. E. and Dietrich, S. (2014). Dact genes are chordate specific regulators at the intersection of Wnt and Tgf-β signaling pathways. *BMC Evol. Biol.* **14**, 157.

Sela-Donenfeld, D. and Kalcheim, K. (1999). Regulation of the onset of neural crest emigration by coordinated activity of BMP4 and Noggin in the dorsal neural tube. *Development* **126**, 4749-4762.

Steventon, B., Araya, C., Linker, C., Kuriyama, S. and Mayor, R. (2009). Differential requirements of BMP and Wnt signalling during gastrulation and neurulation define two steps in neural crest induction. *Development* **136**, 771-779.

Streit, A. and Stern, C. D. (1999). Establishment and maintenance of the border of the neural plate in the chick: involvement of FGF and BMP activity. *Mech. Dev.* **82**, 51-66.

Ten Berge, D., Koole, W., Fuerer, C., Fish, M., Eroglu, E. and Nusse, R. (2008). Wnt signaling mediates self-organization and axis formation in embryoid bodies. *Cell Stem Cell* **3**, 508-518.

Wang, S., Dong, Y., Zhang, Y., Wang, X., Xu, L., Yang, S., Li, X., Dong, H., Xu, L., Su, L. et al. (2015). DACT2 is a functional tumor suppressor through inhibiting Wnt/β-catenin pathway and associated with poor survival in colon cancer. *Oncogene* **34**, 2575-2585.

Wen, J., Chiang, Y. J., Gao, C., Xue, H., Xu, J., Ning, Y., Hodes, R. J., Gao, X. and Chen, Y.-G. (2010). Loss of Dact1 disrupts planar cell polarity signaling by altering dishevelled activity and leads to posterior malformation in mice. *J. Biol. Chem.* **285**, 11023-11030.

Yamamoto, H., Ihara, M., Matsuura, Y. and Kikuchi, A. (2003). Sumoylation is involved in β-catenin-dependent activation of Tcf-4. *EMBO J.* **22**, 2047-2059.

Zhang, L., Gao, X., Wen, J., Ning, Y. and Chen, Y.-G. (2006). Dapper 1 antagonizes Wnt signaling by promoting dishevelled degradation. *J. Biol. Chem.* **281**, 8607-8612.

Zhang, M., Mahoney, E., Zuo, T., Manchanda, P. K., Davuluri, R. V. and Kirschner, L. S. (2014). Protein kinase A activation enhances β-catenin transcriptional activity through nuclear localization to PML bodies. *PLoS ONE* **9**, e109523.